Available online at www.sciencedirect.com
ScienceDirect
Journal of Molecular Catalysis A: Chemical 282 (2008) 129–135
JOURNAL OF MOLECULAR CATALYSIS A: CHEMICAL
www.elsevier.com/locate/molcata

Hydrogen production by partial oxidation of methanol over ZnO-promoted Au/Al_2O_3 catalysts

Feg-Wen Chang *, Szu-Chia Lai, L. Selva Roselin

Department of Chemical and Materials Engineering, National Central University, Chungli 32001, Taiwan

Received 8 August 2007; received in revised form 22 November 2007; accepted 2 December 2007
Available online 8 December 2007

Abstract

Production of hydrogen by partial oxidation of methanol (POM) ($CH_3OH + 0.5O_2 \rightarrow 2H_2 + CO_2$) was investigated over Au/Al_2O_3 and ZnO-promoted Au/Al_2O_3 ($Au/ZnO/Al_2O_3$) catalysts. The catalysts were prepared by deposition–precipitation method and characterized by XRD, TEM and TPR analyses. The addition of ZnO to Au/Al_2O_3 resulted in higher catalytic activity for POM to produce hydrogen. The activity of the catalyst for hydrogen formation increases with increasing the addition of ZnO, and it reaches a maximum when the atomic ratio of Zn to Au is 5/1. The main role of ZnO is associated with the progressive formation of smaller Au particles, which comprise active oxygen species for oxidation of methanol. Catalytic activity of $Au/ZnO/Al_2O_3$ catalyst at various calcination temperatures shows that the uncalcined sample exhibits higher activity for hydrogen formation. The catalytic performance at various reaction temperatures shows that methanol conversion and hydrogen selectivity are increased with rise in reaction temperature. Other by-products formed are traces of methyl formate at low temperatures and traces of methane at high temperatures along with lesser amount of carbon monoxide.

Keywords: Au/Al_2O_3 catalyst; ZnO; Promoter effect; Partial oxidation of methanol; Hydrogen

1. Introduction

The proton exchange membrane fuel cell (PEMFC) can generate electricity without polluting the environment [1,2]. In this system hydrogen fuel is oxidized over Pt electrode and electric energy is generated with H_2O being the only reaction product. The lack of infrastructure for hydrogen production and distribution, as well as the current cost of hydrogen production from nuclear or renewable energy has led to consider on-board hydrogen generation from various hydrocarbons. Partial oxidation of methanol (POM) offers a potential process of producing hydrogen through an exothermic reaction. In the previous studies it was reported that supported copper, palladium, platinum and gold catalysts are active for hydrogen generation from methanol by POM [3–12].

Presently, great attention is paid on supported gold catalysts due to their high activity at low temperatures in a number of important reactions [10,13–16]. The performance of gold catalysts is known to be highly dependent on the combination of two factors, namely the size of the gold crystallites [13,17,18] and the nature of the support. Several studies have indeed shown that the preparation method is a key parameter that strongly affects the size of gold particles and thus the catalytic activity. Haruta [19] indicated that deposition–precipitation (DP) technique has the advantage over co-precipitation (CP), in that all of the active components remain on the surface and none of the active gold component is buried within it. Au catalysts supported on reducible transition metal oxide is more active than those supported on non-reducible metal oxides [20,21]. Moderately active catalysts are obtained by using Al_2O_3 as support for CO oxidation [22]. The presence of transition metal oxide is beneficial for the improvement of catalytic performance of Au/Al_2O_3 catalysts for low temperature CO oxidation [22–24], CH_4 oxidation [23], reduction of N_2O [25], combustion of VOCs [26], WGS reaction [16] and total oxidation of propene [27]. Grisel et al. [23] reported that metal oxide (MO_x) additives stabilize gold nanoparticles on alumina and the resulting catalyst is thermally resistant up to 700 °C. The same research group has also studied the total oxidation of propene over alkali (earth) metal oxide-doped Au/Al_2O_3 catalyst [27]. The addition of several

* Corresponding author. Tel.: +886 3 4227151x34202; fax: +886 3 4252296.
E-mail address: fwchang@cc.ncu.edu.tw (F.-W. Chang).

1381-1169/$ – see front matter © 2007 Elsevier B.V. All rights reserved.
doi:10.1016/j.molcata.2007.12.002

metal oxide additives including Cr, Mn, Fe, Co, Ni, Cu and Zn enhances the catalytic activity and diminishes the temperature of oxidation of CO and CH_4 [28]. The role of these additives was in oxygen activation via Mars and Van Krevelen-type mechanism and to stabilize the gold particle size against sintering. Among different metal oxide additives, ZnO plays a vital role in the development of high catalytic activity. ZnO was used as promoter for promoting the catalytic activity of Cu–Al catalysts for partial oxidation of methanol and steam reforming of methanol [5,6,29]. The enhanced activity of the catalyst was attributed to the behavior of ZnO as a Bronsted base [29]. An alternative view has been proposed by Grunwaldt et al. [30], according to which the defective ZnO causes change in the particle morphology of the copper, thereby enhances the activity.

The aim of the present study was to investigate the effect of ZnO on the activity of Au/Al_2O_3 catalysts in partial oxidation of methanol (POM) to produce hydrogen. The influence of calcination temperature and reaction temperature on the activity of ZnO-promoted Au/Al_2O_3 ($Au/ZnO/Al_2O_3$) catalysts was also investigated.

2. Experimental

2.1. Catalyst preparation

The Au/Al_2O_3 catalyst sample with an initial Au loading of 1 wt.% was prepared by the deposition–precipitation (DP) technique [31]. An aqueous solution of $HAuCl_4{\cdot}3H_2O$ (99.99%, Alfa Aesar) was heated to 343 K and the pH was adjusted to 8.0 by addition of small amount of 0.1 N NaOH. This is followed by the addition of Al_2O_3 support (99% Merck). The slurry was then aged at 343 K for 2 h. The precipitates were filtered and washed with deionized water several times until the disappearance of chloride and sodium ions. The samples were dried overnight at 373 K and subsequently calcined in air at different temperatures for 4 h.

$Au/ZnO/Al_2O_3$ catalyst sample with various Zn:Au atomic ratios, viz. 1:1, 3:1, 5:1 and 7:1 were prepared by the same method using aqueous solution of $Zn(NO_3)_2{\cdot}3H_2O$ and $HAuCl_4{\cdot}3H_2O$. The samples were dried overnight at 373 K and were calcined in air at different temperatures for 4 h.

2.2. Catalyst characterization

X-ray diffraction measurements (XRD) were performed using a Schimadza XD-5 diffractometer operated at 40 kV and 30 mA using Cu Kα radiation with a wavelength of 1.5406 Å. The scanning angle has been set (Bragg angle 2θ) from 20° to 70° at a rate of 0.05°/s.

The transmission electron microscopy (TEM) analyses were performed on a JEOL JEM-2000FX II, the operating voltage was set at 160 kV. Samples were mounted on a microgrid carbon polymer supported on a copper grid by placing a few droplets of a suspension of ground sample in ethanol on the grid, followed by drying at 333 K.

Temperature-programmed reduction (TPR) of the catalyst was performed in a U-shaped microreactor made of quartz, surrounded with a furnace controlled by a programmed heating system. Prior to the TPR experiment, 40 mg of the catalyst sample was pretreated under flowing Ar (20 ml/min) at room temperature for 1 h. After the pretreatment, a reducing gas composed of 5% H_2 plus 95% Ar was employed at a flow rate of 20 ml/min, with a heating ramp of 10 K/min from 323 to 773 K. The amount of the consumed H_2 was determined by a thermal conductivity detector (TCD).

2.3. Partial oxidation of methanol

Hydrogen production by partial oxidation of methanol was studied over Au/Al_2O_3 and $Au/ZnO/Al_2O_3$ catalysts. The reaction was carried out at atmospheric pressure and at temperatures between 448 and 548 K, using a U-shaped microreactor made of quartz (i.d. = 4 mm) [10]. The reactor was located in a programmable furnace with a type K thermocouple placed in the center of the catalyst bed. The Ar and O_2 were transported by Brooks 5850E mass flow meter with a precision controller (Protec Instrument Co. Ltd. Model: PC-540) to control the total flow rate at 60 ml/min. The reaction products were analyzed on-line using two gas chromatographs (GC) equipped with thermal conductivity detector and porapak Q and carbosieve S-II columns.

3. Results and discussion

3.1. XRD

Fig. 1 shows the X-ray diffraction patterns of $Au/ZnO/Al_2O_3$ catalyst with different Zn/Au ratios. It can be seen that at lower additions of ZnO (Zn/Au = 1/1, 3/1 and 5/1) (Fig. 1b–d), the diffraction line corresponds to ZnO was not observed. However, at higher addition of ZnO (Zn/Au = 7/1), the diffraction line corresponds to ZnO was observed (Fig. 1e). The absence of peaks at lower Zn/Au ratios would imply that in these catalysts the ZnO species are dispersed uniformly over the support. In addition, the

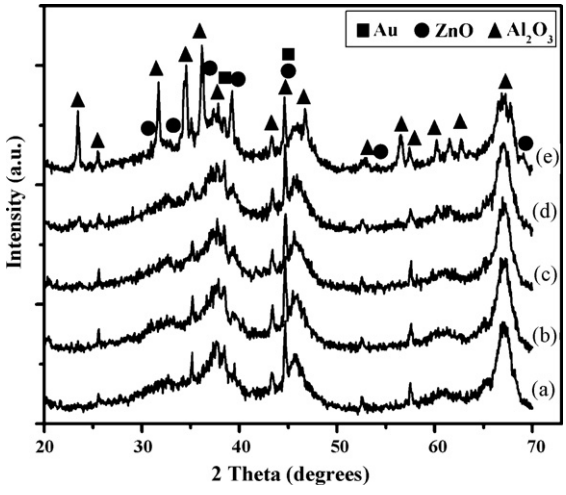

Fig. 1. XRD patterns of uncalcined $Au/ZnO/Al_2O_3$ catalyst with various Zn/Au atomic ratios. (a) Zn/Au = 0/1; (b) Zn/Au = 1/1; (c) Zn/Au = 3/1; (d) Zn/Au = 5/1; (e) Zn/Au = 7/1.

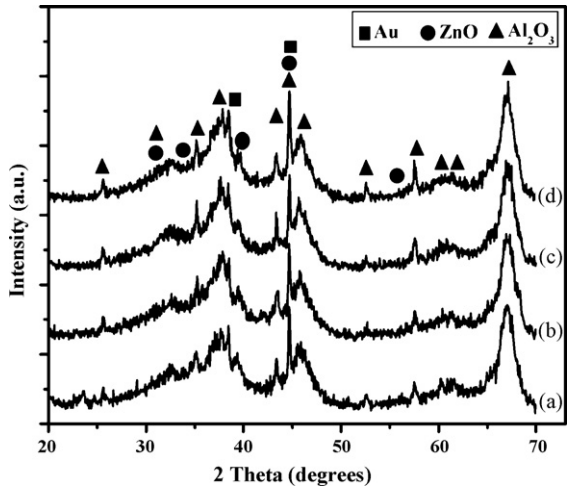

Fig. 2. XRD patterns of $Au/ZnO/Al_2O_3$ catalyst calcined at different temperatures: (a) uncalcined, dried at 373 K; (b) calcined at 573 K; (c) calcined at 673 K; (d) calcined at 873 K (Zn/Au atomic ratio, 5/1).

weight percentage of ZnO might be under the detection limit of XRD analysis. In the sample containing higher amount of ZnO (Zn/Au = 7/1) there was an enhanced crystallization of alumina support was observed. In these samples weak diffraction lines of gold are merged with the intense peaks of alumina support. In particular, the $2\theta = 38.2^\circ$ (Au(1 1 1)) and $2\theta = 44.4^\circ$ (Au (2 0 0)) are superimposed by a strong alumina peak at $2\theta = 37.7^\circ$ and $2\theta = 44.6^\circ$. Other characteristic peak for gold, particularly at 64.5° (Au (2 2 0)) was not observed. This is probably due to the presence of small Au particles. Fig. 2 shows the X-ray diffraction patterns of the $Au/ZnO/Al_2O_3$ catalyst (Zn/Au ratio, 5/1) calcined at different calcination temperatures. The peak intensity corresponding to the support (Al_2O_3) was increased with increasing calcination temperature indicating the increased crystallization of the support. The peak intensity corresponding to gold was increased with rise in calcination temperature, which indicates that the particle size of gold in the catalysts was increased as a result of sintering. Since the gold reflections are superimposed by the support, determination of particle size of gold from X-ray line broadening was not attempted.

3.2. TEM

Table 1 shows the average particle size of gold in $Au/ZnO/Al_2O_3$ catalyst with various Zn/Au ratios dried at 373 K. The addition of zinc oxide up to Zn/Au ratio of 5/1 decreased the average gold particle size. Further addition of ZnO (Zn/Au = 7/1) led to increase in Au particle size. The particle size of Au in Au/Al_2O_3 was 4.9 nm and in $Au/ZnO/Al_2O_3$ with different Zn/Au ratios of 1/1, 3/1, 5/1 and 7/1 was 4.8, 3.5, 3.0 and 3.2 nm, respectively. Grisel and Nieuwenhuys [28] and Bethke and Kung [32] have also observed smaller Au particles by the addition of alkali earth metal oxides in Au/Al_2O_3 catalyst. The decrease in particle size may originate from redistribution of Au in solution during ZnO deposition [28]. In this, inclusion of ZnO on the surface of the support leads to smaller Au particle. However, at higher amount of ZnO addition leads to agglomeration of small

Table 1
Average size of gold in Au/Al_2O_3 and $Au/ZnO/Al_2O_3$ catalysts

Catalyst	Calcination temperature (K)	Zn/Au atomic ratio	Average Au particle size (nm)[a]
Au/Al_2O_3	Uncalcined	0/1	4.9
$Au/ZnO/Al_2O_3$	Uncalcined	1/1	4.8
$Au/ZnO/Al_2O_3$	Uncalcined	3/1	3.5
$Au/ZnO/Al_2O_3$	Uncalcined	5/1	3.0
$Au/ZnO/Al_2O_3$	Uncalcined	7/1	3.2
Au/Al_2O_3	573	0/1	5.3
$Au/ZnO/Al_2O_3$	573	5/1	3.8
$Au/ZnO/Al_2O_3$	673	5/1	5.2
$Au/ZnO/Al_2O_3$	873	5/1	8.8
$Au/ZnO/Al_2O_3$[b]	573	5/1	7.4

[a] Calculated from TEM data.
[b] After POM at 548 K for 2 h.

gold particles. Examination of the catalyst after calcination indicates that the sintering behavior was found to depend strongly on the metal oxide additive. The Au particle was sintered more easily in the case of Au/Al_2O_3 than in $Au/ZnO/Al_2O_3$ catalysts. The average particle size of Au in Au/Al_2O_3 and $Au/ZnO/Al_2O_3$ after calcination at 573 K was 5.3 and 3.8 nm, respectively. This result suggests that sintering of small Au particles was inhibited by the addition of ZnO. Kang and Wan [33] have also observed similar stabilization of Au particles in Au/zeolite-Y catalyst by the addition of FeO_x. But, at higher calcination temperature large sized Au particles were observed in $Au/ZnO/Al_2O_3$ catalysts. The mean gold particle size after calcination at 673 and 873 K are 5.2 and 8.8 nm, respectively. Therefore, when the calcination temperature was above 673 K strong sintering occurs resulted in large sized Au particles. Previous study shows that the small Au particles tend to sinter during heat treatments above 673 K [28]. The $Au/ZnO/Al_2O_3$ catalysts after catalytic test at 548 K were collected and well-mixed and characterized for particle size analysis. It revealed that there was a change in the average particle size of the gold in the samples exposed to the POM reaction at 548 K. The mean Au particle size was increased from 3.8 to 7.4 nm during catalytic test. This indicates that during POM, aggregation of smaller Au particles resulted in large sized Au crystallites. The present study suggests that the small Au particles in $Au/ZnO/Al_2O_3$ catalyst are sintered considerably after calcination at 673 K and after catalytic test. Therefore the involvement of ZnO in preserving the Au particle size during heat treatment was found to be lesser in $Au/ZnO/Al_2O_3$ catalyst at high temperatures.

3.3. TPR

Fig. 3 illustrates the TPR patterns of Au/Al_2O_3 catalyst sample and $Au/ZnO/Al_2O_3$ catalyst sample with various additions of ZnO. It can be seen that in all the samples a reduction peak for Au_xO_y was observed at 505 K. In addition to the peak for reduction of gold oxide, the catalyst samples with high ZnO content an additional peak in the low temperature region was observed. The low temperature peak has been assigned to the reduction of oxygen species on the nanosize gold particles [34]. It is clearly seen that the low temperature peak shifted to higher

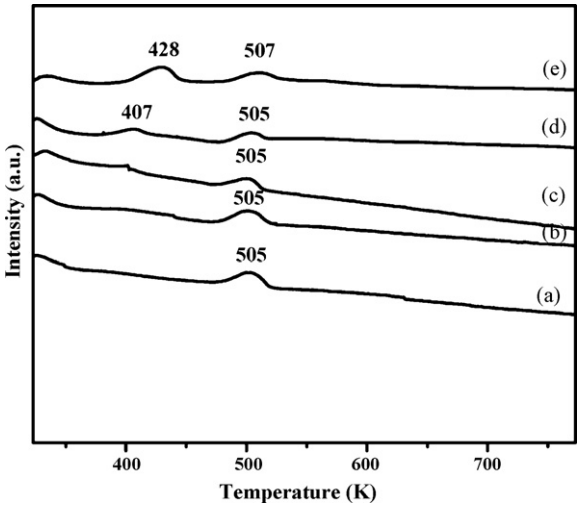

Fig. 3. TPR patterns of uncalcined $Au/ZnO/Al_2O_3$ catalyst with various Zn/Au atomic ratios. (a) Zn/Au = 0/1; (b) Zn/Au = 1/1; (c) Zn/Au = 3/1; (d) Zn/Au = 5/1; (e) Zn/Au = 7/1.

temperature with higher content of ZnO. This indicates that in these samples the oxygen species strongly bound on the catalyst surfaces, which are difficult to reduce. The TPR patterns of $Au/ZnO/Al_2O_3$ catalyst at different calcination temperatures are shown in Fig. 4. In the figure, the uncalcined catalyst sample exhibits two peaks. The peak at 407 K corresponds to the reduction of oxygen species adsorbed on the nanosize gold particles. The other peak at 505 K corresponds to the reduction of oxidized gold species. After calcination, the peak corresponding to the reduction of oxidized gold species were not observed. This indicates that the oxidized gold species were reduced to metallic gold during calcination. In the sample after calcination 573 K, the low temperature reduction peak for oxygen species on the nanosize gold particles was observed as small shoulder. However, at higher calcination temperatures (673 and 873 K) these peaks were not observed. This denotes the absence of

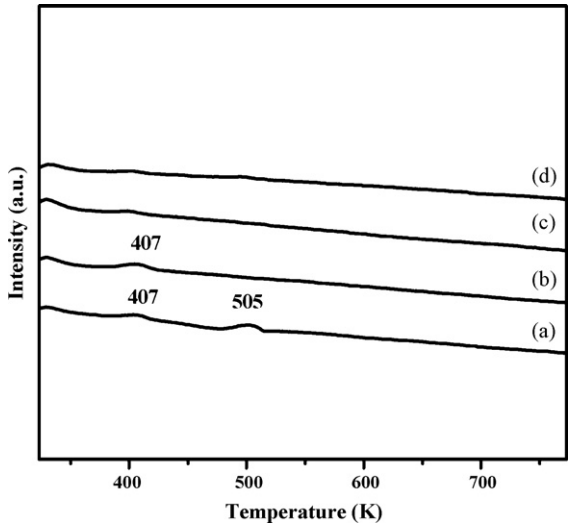

Fig. 4. TPR patterns of $Au/ZnO/Al_2O_3$ catalyst calcined at different temperatures: (a) uncalcined, dried at 373 K; (b) calcined at 573 K; (c) calcined at 673 K; (d) calcined at 873 K (Zn/Au atomic ratio, 5/1).

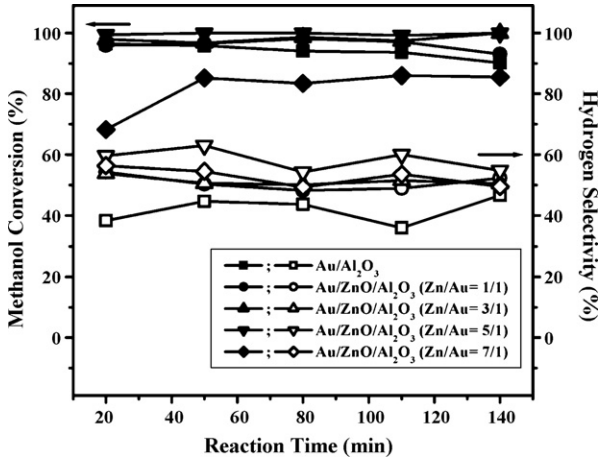

Fig. 5. Effect of Zn/Au atomic ratio on methanol conversion and hydrogen selectivity for POM over uncalcined $Au/ZnO/Al_2O_3$ catalysts (uncalcined, dried at 373 K; reaction temperature, 523 K).

adsorbed oxygen species on the surface of the nanogold particles. This might be due to the presence of larger Au particles, which are difficult to adhere oxygen molecules on the Au surface. TEM analysis confirmed large Au particle in the sample after calcination at 673 and 873 K (Table 1).

3.4. Catalytic activity

The catalytic activity and product distribution in methanol partial oxidation (POM) over $Au/ZnO/Al_2O_3$ catalysts was studied with oxygen/methanol feed ratio of 0.5. Hydrogen and carbon dioxide were the main products. Other by-products formed are water, carbon monoxide, methane and methyl formate.

Fig. 5 shows methanol conversion and hydrogen selectivity during POM at 523 K over uncalcined Au/Al_2O_3 catalyst and $Au/ZnO/Al_2O_3$ catalyst with different Zn/Au ratios. It can be seen that a remarkable improvement of catalytic activity in terms of hydrogen selectivity was observed by the addition of ZnO to Au/Al_2O_3. Furthermore, the activity of the catalyst for hydrogen formation increased continuously with increase in the amount of ZnO and it reached a maximum when the atomic ratio of Zn to Au is 5/1. At higher amount of ZnO addition, the catalytic activity of the $Au/ZnO/Al_2O_3$ catalyst was decreased. The above results show that appropriate addition of Zn is helpful to improve the activity of the catalyst for hydrogen generation. Similar enhancement in catalytic activity was also observed for Au/Al_2O_3 catalyst by the addition of ZnO after calcination at 573 K (Fig. 6). The enhancement of activity by ZnO addition has also been observed in supported copper catalysts for POM to produce hydrogen [5,6,35]. Many authors discussed a number of models, which could account for the observed improved activity over Cu/Al_2O_3 catalysts upon addition of ZnO [5,6,29,30]. In the present study, the observed improved activity is directly correlated with the average Au particle size (Table 1). Since, the addition of ZnO stabilizes small Au particles, close contact between Au and ZnO is expected. It is generally accepted that small Au particles are beneficial for low temperature CO

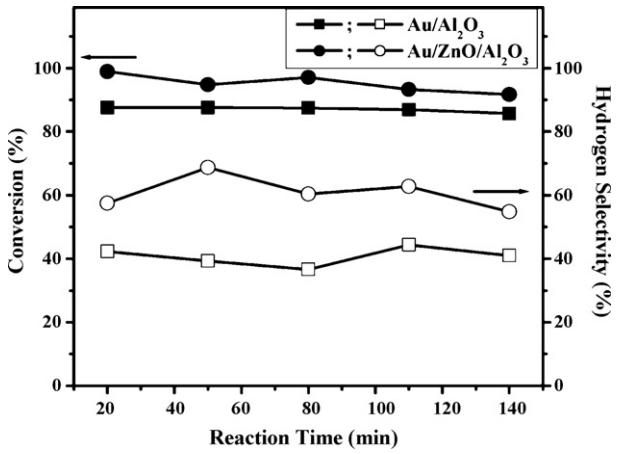

Fig. 6. Effect of ZnO addition on methanol conversion and hydrogen selectivity for POM over calcined Au/Al_2O_3 catalysts (Zn/Au atomic ratio, 5/1; calcination temperature, 573 K; reaction temperature, 523 K).

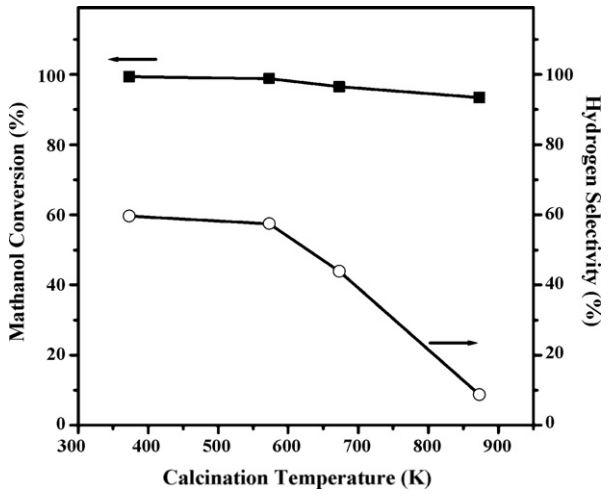

Fig. 7. Effect of calcination temperature on methanol conversion and hydrogen selectivity for POM over $Au/ZnO/Al_2O_3$ catalysts (Zn/Au atomic ratio, 5/1; reaction temperature, 523 K; reaction time, 20 min).

oxidation [20], CH_4 oxidation [23] and methanol partial oxidation [10,11]. It is attributed that in small sized Au contained catalysts, either the presence of large total Au/support interface [20,36,37] or the presence of special sites such as coordinately unsaturated Au surface atoms [38], a special electronic structure of very small Au particles [39], or ionic Au species [32,40] or active oxygen species are particularly present on small Au particles [41]. Both Au/support interface and the possible presence of active oxygen species are relatively more abundant when dealing with small Au particles. The TPR patterns of $Au/ZnO/Al_2O_3$ uncalcined sample with Zn/Au ratios of 5/1 and 7/1 (Fig. 3d and e) showed a reduction peak corresponding to surface adsorbed oxygen species on the nanogold particles. Another important characteristic of ZnO is its behavior of Bronsted base, which can accept the spillover proton obtained from the dissociative adsorption of methanol and stabilize the methoxy species [29]. Therefore, it is believed that the role of ZnO in promoting POM is in two ways. The first way is to stabilize small Au particles leading to close contact between Au and ZnO. The small Au particle adhere active oxygen on the surface of the catalyst [41]. The second factor is owing to the behavior of ZnO as Bronsted base, which facilitates the O–H bond cleavage in methanol and forms methoxy species and these species are adsorbed at or near the Au-support perimeter. It was reported that the perimeter interface is the suited place for reaction to take place [20]. As a result, no migration of activated oxygen and the methoxy species are necessary, thereby promote the activity of the catalyst. Therefore, the ZnO-promoted catalysts ensure its contribution towards the O–H bond cleavage and also increase the availability of reactive oxygen species on nanogold particles. The $Au/ZnO/Al_2O_3$ catalysts calcined at 673 and 873 K contain large sized Au particles, which showed much lower activity. This proves that apart from O–H bond cleavage by ZnO, presence of small Au particles contain reactive oxygen species on the surface of the catalyst, is the major factor that could influence the activity of the catalyst. In Fig. 5, the catalyst sample with Zn/Au ratio 5/1 showed higher activity than the catalyst with Zn/Au ratio 7/1. This is due to the presence of large sized Au particles in the catalyst sample with Zn/Au ratio 7/1 (Table 1). In addition, the TPR study showed that in the sample with Zn/Au ratio 5/1 the reduction peak for oxygen species adsorbed on the nanogold species are reduced at lower temperature than those in the catalyst sample with Zn/Au ratio 7/1. This indicates that the reactive oxygen species are easily assessable for reaction in the catalyst sample with Zn/Au ratio 5/1. Besides, at higher amount of ZnO (at Zn/Au ratio 7/1), parts of Au may be covered by ZnO patches, reducing the amount of active Au surface available for the reaction. Therefore, optimum Zn/Au ratio in $Au/Zno/Al_2O_3$ catalyst for POM to produce hydrogen was fixed at 5/1.

Fig. 7 shows the effect of calcination temperature on methanol conversion and hydrogen selectivity for POM over $Au/ZnO/Al_2O_3$ catalysts. With increase in calcination temperature a slight decrease in methanol conversion was observed. However, larger difference in hydrogen selectivity was observed at different calcination temperatures. The hydrogen selectivity was decreased with increase in calcination temperature. The decrease was found to be higher beyond 573 K. The catalyst calcined at 673 K showed lower activity and the sample calcined at 873 K showed negligible activity for hydrogen formation. The higher activity of uncalcined catalyst sample and the sample calcined at 573 K can be correlated with the particle size of Au. TEM revealed that the uncalcined catalyst sample and the sample calcined at 573 K exhibited smaller Au particles compared to the catalyst samples calcined beyond 573 K (Table 1). The drop in activity for the sample beyond 573 K is due to the presence of larger Au particles. It was reported that, large sized gold particles accelerate the oxidation of hydrogen [42]. Since the $Au/ZnO/Al_2O_3$ catalyst without calcination itself showed higher activity for POM, the same has been used for further study.

Fig. 8 shows the methanol conversion and hydrogen selectivity for POM over $Au/ZnO/Al_2O_3$ (Zn/Au = 5/1) catalyst at reaction temperatures between 448 and 548 K. It can be seen that complete conversion of oxygen was observed throughout the temperature studied. Methanol conversion was almost same

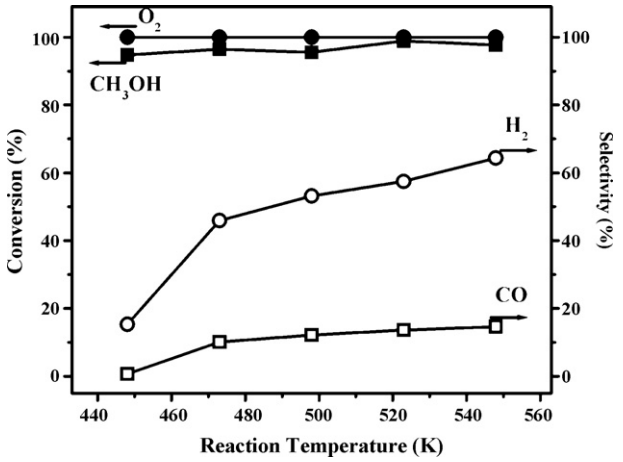

Fig. 8. Effect of reaction temperature on methanol conversion, oxygen conversion, hydrogen selectivity and CO selectivity for POM over $Au/ZnO/Al_2O_3$ catalysts (Zn/Au atomic ratio, 5/1; uncalcined, dried at 373 K; reaction time, 20 min).

and was close to 100% (94–98%). However, distribution of products is varying with reaction temperature. Methyl formate ($HCOOCH_3$) was formed only in trace quantities at reaction temperature below 523 K. Methane formed in small amounts only at high temperatures. Other formate species containing products, such as formaldehyde and formic acid, which are often formed by reactions of methanol in the presence of copper catalysts could not be detected under the reaction conditions employed. Manzoli et al. [43] showed, by FTIR studies that gold cannot activate the formation of formaldehyde and formic acid, whereas the copper catalyst can execute. In Fig. 8, as oxygen was completely consumed throughout the reaction temperature studied, the conversion trend suggests that, along with the POM reaction, other methanol consumption reactions have taken place. During partial oxidation, as discussed in our previous studies [10,11], initially methanol quickly consumes excess oxygen leading to highly exothermic methanol combustion (MC) reaction (Eq. (1)) to occur and produce water and carbon dioxide.

$$CH_3OH + 1.5O_2 \rightarrow 2H_2O + CO_2 \quad (1)$$

The high stoichiometric amount of O_2 required for the total oxidation of methanol entails a fast decrease of the O_2 content in the gas. This decrease in the oxidizing potential of the gas phase, together with the excess of energy, implies a progressive removal of surface oxygen species, which favors the dehydrogenation pathway under substoichiometric amounts of surface oxygen. Methanol dehydrogenates to produce methyl formate and hydrogen (Eq. (2)) [44].

$$2CH_3OH \leftrightarrow HCOOCH_3 + 2H_2 \quad (2)$$

The selectivity towards methyl formate is decreased with reaction temperature and attains zero at 523 K. This may be due to further decomposition into methanol and CO (Eq. (3)) [5].

$$HCOOCH_3 \leftrightarrow CO + CH_3OH \quad (3)$$

When all oxygen available for oxidation has been consumed, the excess of methanol is converted through the endothermic decomposition pathway (MD) (Eq. (4)) [32].

$$CH_3OH \rightarrow 2H_2 + CO \quad (4)$$

CO can be detected beyond 473 K. No measurable amount of CO was observed at the reaction temperature of 448 K. This may be due to the product formation by the exothermic water gas shift reaction (WGS) (Eq. (5)).

$$CO + H_2O \rightarrow H_2 + CO_2 \quad (5)$$

The presence of CO in the reaction product with increasing temperature is due to reaction in Eqs. (3) and (4). However, the CO selectivity was lesser than those observed in $Cu/ZnO/Al_2O_3$ catalysts [29]. This is due to smaller Au contained in the catalyst, which consequently enhanced the activity towards direct oxidation of CO in the presence of oxygen. The supported gold catalysts are active for low temperature CO oxidation (Eq. (6)).

$$CO + 0.5O_2 \rightarrow CO_2 \quad (6)$$

In addition to that, as water is produced by MC promote WGS, which in turn leads to minimization of CO in the product gas. Ghiotti and Boccuzzi [45] indicated that the WGS reaction may be enhanced over Zn-promoted catalysts. It is possible to eliminate CO completely if the CO oxidation and WGS reactions can be driven to completion. However, there seems to be unfavorable equilibrium for CO consumption. This is because of the presence of high amount of H_2 and CO_2 in the product gas compared to the extremely small amount of CO. This scenario activates the reverse water gas shift (RWGS), which leads to presence of some amount of CO in the product gas (~10%). In the previous studies it was reported that the CO selectivity increased with increase in reaction temperature [8–11]. However, in the present study, beyond 473 K, a steady amount of CO was observed. This is because of the coexistence of MD, WGS, RWGS and CO oxidation. In the product stream, other undesired by-product observed was small amount of methane. In our previous studies we have observed small amount of methane by-product during POM over Au/TiO_2 catalyst [10]. Hydrogen dissociates on nanosized gold producing atomic hydrogen, which may react with methanol and produce methane [46]. Rupprechter [47] suggested another route for methane formation during POM as direct hydrogenation of CO in excess of hydrogen ($CO + xH \leftrightarrow CH_xO$), followed by C–O bond scission ($CH_xO \leftrightarrow CH_x + O$) and hydrogenation to methane. The over all reaction route suggests that generation of hydrogen occurred as a result of combination of various reactions during partial oxidation condition. They are POM, SRM, MD and WGS reactions. The hydrogen selectivity increased from 15 to 64% with increase in reaction temperature from 448 to 548 K. The unfavorable effect of the occurrence of methanol deep oxidation, hydrogen oxidation, RWGS and methane formation is the subtraction of hydrogen to the main product. However, it is relevant to stress that CO selectivity is much lower than those observed over supported copper and palladium catalysts.

4. Conclusions

The present study shows that addition of ZnO to Au/Al_2O_3 resulted in higher catalytic activity for POM to produce hydrogen. This promoting effect of ZnO can be associated with the progressive formation of smaller particles of Au highly dispersed on the surface, which comprise active oxygen species for oxidation of methanol. Catalytic activity of $Au/ZnO/Al_2O_3$ catalyst at various calcination temperatures shows that the uncalcined sample exhibits higher activity for hydrogen formation. The catalytic performance at various reaction temperatures shows that with increasing the temperature from 448 to 548 K methanol conversion increases from 94 to 98% and hydrogen selectivity increases from 15 to 64%. Other by-products formed are traces of methyl formate at low temperatures and traces of methane at high temperatures along with lesser amount of carbon monoxide.

Acknowledgement

The authors express thanks to the Ministry of Economical Affairs of Taiwan for its financial support under contract number 93-EC-17-A-09-S1-022.

References

[1] B. Lindner, K. Sjomstrom, Fuel 63 (1984) 1485.
[2] J. Appleby, F.R. Foulkes, Fuel Cell Handbook, Van Nostrand Reinhold, New York, 1989, p.177.
[3] L. Alejo, R. Lago, M.A. Peña, J.L.G. Fierro, Appl. Catal. A 162 (1997) 281.
[4] J. Agrell, M. Boutonnet, J.L.G. Fierro, Appl. Catal. A 253 (2003) 213.
[5] R.M. Navarro, M.A. Peña, J.L.G. Fierro, J. Catal. 212 (2002) 112.
[6] Z. Wang, J. Xi, W. Wang, G. Lu, J. Mol. Catal. A 191 (2003) 123.
[7] L.A. Espinosa, R.M. lago, M.A. Pena, J.L.G. Fierro, Top. Catal. 22 (2003) 245.
[8] J. Agrell, G. Germani, S.G. Järås, M. Boutonnet, Appl. Catal. A 242 (2003) 233.
[9] M.L. Cubeiro, J.L.G. Fierro, Appl. Catal. A 168 (1998) 307.
[10] F.-W. Chang, H.-Y. Yu, L.S. Roselin, H.-C. Yang, Appl. Catal. A 290 (2005) 138.
[11] F.-W. Chang, H.-Y. Yu, L.S. Roselin, H.-C. Yang, T.-C. Ou, Appl. Catal. A 302 (2006) 157.
[12] R. Ubago-Peĭrez, F. Carrasco-Marıĭn, C. Moreno-Castilla, Catal. Today 123 (2007) 158.
[13] M. Haruta, T. Kobayashi, H. Sano, N. Yamada, Chem. Lett. 2 (1987) 405.
[14] T. Hayashi, K. Tanaka, M. Haruta, J. Catal. 178 (1998) 566.
[15] G.J. Hutchings, Catal. Today 72 (2002) 11.
[16] T. Tabakova, V. Idakiev, D. Andreeva, I. Mitov, Appl. Catal. A 202 (2000) 91.
[17] M. Haruta, Catal. Today 36 (1997) 153.
[18] D. Wang, Z. Hao, D. Cheng, X. Shi, C. Hu, J. Mol. Catal. A 200 (2003) 229.
[19] M. Haruta, Catal. Surv. Jpn. 1 (1997) 61.
[20] M. Haruta, S. Tsubota, T. Kobayashi, H. Kageyma, M.J. Genet, B. Delmon, J. Catal. 144 (1993) 175.
[21] M.M. Schubert, S. Hackenberg, A.C. van Veen, M. Muhler, V. Plzak, R.J. Behm, J. Catal. 197 (2001) 113.
[22] R.J.H. Grisel, B.E. Nieuwenhuys, J. Catal. 199 (2001) 48.
[23] R.J.H. Grisel, J.J. Slyconish, B.E. Nieuwenhuys, Top. Catal. 16/17 (2001) 425.
[24] R.J.H. Grisel, P.J. Kooyman, B.E. Nieuwenhuys, J. Catal. 191 (2000) 430.
[25] A.C. Gluhoi, M.A.P. Dekkers, B.E. Nieuwenhuys, J. Catal. 219 (2003) 197.
[26] M.A. Centeno, M. Paulis, M. Montes, J.A. Odriozola, Appl. Catal. A 234 (2002) 65.
[27] A.C. Gluhoi, N. Bogdanchikova, B.E. Nieuwenhuys, J. Catal. 232 (2005) 96.
[28] R.J.H. Grisel, B.E. Nieuwenhuys, Catal. Today 64 (2001) 69.
[29] R.O. Idem, N.N. Bakhshi, Ind. Eng. Chem. Res. 34 (1995) 1548.
[30] J.D. Grunwaldt, A.M. Molenbroek, N.Y. Topsøe, H. Topsøe, B.S. Clausen, J. Catal. 194 (2000) 452.
[31] E.D. Park, J.S. Lee, J. Catal. 186 (1999) 1.
[32] G.K. Bethke, H.H. Kung, Appl. Catal. A 194/195 (2000) 43.
[33] Y.M. Kang, B.Z. Wan, Catal. Today 26 (1995) 59.
[34] V. Idakiev, L. Ilievaa, D. Andreeva, J.L. Blin, L. Gigot, B.L. Sub, Appl. Catal. A 243 (2003) 25.
[35] Z. Wang, W. Wang, G. Lu, Int. J. Hydrogen Energy 28 (2003) 151.
[36] G.R. Bamwenda, S. Tsubota, T. Nakamura, M. Haruta, Catal. Lett. 44 (1997) 83.
[37] S. Tsubota, T. Nakamura, K. Tanaka, M. Haruta, Catal. Lett. 56 (1998) 131.
[38] F. Boccuzzi, G. Cerrato, F. Pinna, G. Strukul, J. Phys. Chem. B 102 (1998) 5733.
[39] M. Valden, X. Lai, D.W. Goodman, Science 281 (1998) 59.
[40] S. Minico, S. Scire, A. Viscio, S. Galvano, Catal. Lett. 47 (1997) 273.
[41] D.Y. Cha, G. Parravano, J. Catal. 18 (1970) 200.
[42] T.V. Choudhary, C. Sivadinarayana, C.C. Chusuei, A.K. Datye, J.P. Fackler, D.W. Goodman, J. Catal. 207 (2002) 247.
[43] M. Manzoli, A. Chiorino, F. Boccuzzi, Appl. Catal. B 57 (2004) 201.
[44] S. Patel, K.K. Pant, J. Power Sources 159 (2006) 139.
[45] G. Ghiotti, F. Boccuzzi, Catal. Rev. Sci. Eng. 29 (1987) 151.
[46] F. Boccuzzi, A. Chiorino, M. Manzoli, D. Ardreeva, T. Tabakova, J. Catal. 188 (1999) 176.
[47] G. Rupprechter, Catal. Today 126 (2007) 3.